Materials Science

http://www.aimspress.com/journal/Materials/

AIMS Materials Science, 4(4): 970-981.
DOI: 10.3934/matersci.2017.4.970
Received: 30 June 2017
Accepted: 24 August 2017
Published: 31 August 2017

*Research article*

# Morphology orientation of comb-like polymers with rigid backbones under the influence of shear fields

**Gaurav Gupta** [1,2], **Varun Danke** [1,2], **Tamoor Babur** [2], **and Mario Beiner** [1,2,*]

[1] Fraunhofer Institut für Mikrostruktur von Werkstoffen und Systemen IMWS, Walter-Hülse-Straße 1, D-06120 Halle (Saale), Germany

[2] Naturwissenschaftliche Fakultät II, Martin-Luther-Universität Halle-Wittenberg, Heinrich-Damerow-Str. 4, D-06120 Halle (Saale), Germany

[*] **Correspondence:** Email: mario.beiner@imws.fraunhofer.de; Tel: +49-345-5589247; Fax: +49-345-5589101.

**Abstract:** The influence of shear fields on the packing behavior and morphology orientation are studied for two comb-like polymers viz. poly(1,4-phenylene-2,5-didecyloxy terephthalate) (PPDOT) and poly(2,5-didecyloxy-1,4-phenylenevinylene) (DOPPV) with different rigid backbones having C = 10 alkyl carbons per side chain. Crystallographic analysis based on X-ray diffractometry measurements shows that both PPDOT and DOPPV exhibit a long-range ordered layered structure with alternating main chains and alkyl nanodomains and can be characterized by an orthorhombic and monoclinic unit cell respectively. No measurable influence of processing on the unit cell of the individual polymers is observed comparing diffraction data on isotropic (powder) samples and extruded fibers. The main difference between the PPDOT and DOPPV is in the molecular orientation of the backbones in shear aligned fibers as observed from the 2D diffraction patterns. While, for PPDOT the polymer backbones align along the direction of extrusion (fiber axis), for DOPPV the backbones align perpendicular to the extrusion direction. A possible relation between differences in backbone orientation under influence of shear fields for DOPPV and PPDOT and differences in the packing state of the side chains, which are in a crystalline state for DOPPV but in a disordered state for PPDOT, is considered.

**Keywords:** X-ray scattering; crystal structure; oriented fibers; side chain packing; alkyl nanodomains

## 1. Introduction

Among the chemically synthesized functional materials, comb-like polymers with rigid backbones and flexible side chains form an important class with applications in various fields ranging from organic semiconductors [1, 2], light emitting diodes [3], biomedical applications [4], coatings[5] and

light weight components in fiber reinforced composite materials with excellent mechanical properties [6, 7]. The solubility and processability of these comb-like polymers is significantly improved by attaching pendant side chains (containing long methylene sequences) which are otherwise difficult to attain at standard conditions. Morphologically, comb-like polymers typically form layered structures with periodicities in the 1–3 nm range wherein the side chains aggregate to form alkyl nanodomains [7, 8]. A self-assembling process in such systems resulting in the formation of side chain and main chain domains has been termed as nanophase separation [9, 10] and is observed in amorphous and liquid-crystalline polymers with varying side chain lengths. The side chain packing within these alkyl nanodomains can vary depending on various factors viz. the microstructure of the backbone, thermal histroy as well as on the constraints (e.g., areal density in the interface, side chain distance) under which structure formation occurs [10, 11, 12]. In most cases, the rigid backbones consist of ring-like units which tend to form $\pi - \pi$ stacks. It has been highlighted recently that the long range order within the main chain domains and the performance of the materials can be influenced by the packing of the side chains within the alkyl nanodomains [13].

Besides the inherent structural packing, an important aspect that plays a critical role in determining the functional properties of these comb-like polymers is the molecular orientation. Various studies have shown that a preferred molecular orientation can significantly influence the charge transport [14, 15], optical [16, 17], and the mechanical properties [18]. Different techniques like adapted molecular architectures [19], thermal processing [20, 21], epitaxy [22], nanoporous templates [23], electric and magnetic fields (used for semi-crystalline polymers and block copolymers) [24, 25], mechanical stretching [26], friction transfer [27], and high temperature rubbing [28] have been employed to achieve molecular orientation. Despite the number of studies, the effect of shear fields during extrusion on crystal orientation in comb-like polymers is limited. In most cases, oriented comb-like polymers are prepared in ultra-thin supported films with nanoscopic dimensions by special techniques [29, 30]. Otherwise, it is well known that polymer processing techniques like extrusion or injection molding, where strong shear fields do commonly occur, can induce crystal orientation and anisotropic mechanical properties in bulk samples [31]. This effect can seriously influence the mechanical performance of components or semi-finished products. Some studies have been performed on warm-drawn PPAOTs fibers containing oriented crystals [32] with the aim to understand the effect of orientation on mechanical properties, morphology and crystal structure. Recently, the influence of shear fields on the packing states and crystal structure of PPAOT fibers was studied [13]. Similar studies on AOPPVs fibers could serve two purposes in parallel—for obtaining materials with optimized properties but also for reaching a better understanding of crystal structure.

In this work, the structure and orientation of comb-like poly(1,4-phenylene-2,5-didecyloxy terephthalate) (PPDOT) and poly(2,5-didecyloxy-1,4-phenylenevinylene) (DOPPV) with side chain length (C = 10) is investigated. X-ray diffraction measurements on isotropic samples after thermal treatment are combined with 2D scattering measurements on oriented fibers obtained by ram extrusion. Main focus of this work is to study morphology orientation of comb-like polymers with rigid backbones in shear fields.

## 2. Materials and Method

### 2.1. Materials

Poly(1,4-phenylene-2,5-didecyloxy-terephthalate) (PPDOT) and poly(2,5-didecyloxy-1,4-phenylene-vinylene)(DOPPV) with C = 10 alkyl carbons per side chain are studied. The chemical structure of the investigated polymers is shown in Figure 1.

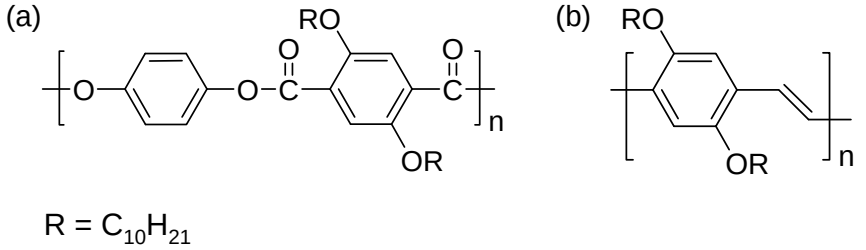


**Figure 1.** Chemical structure of (a) poly(1,4-phenylene-2,5-didecyloxy terephthalate) (PPDOT) and (b) poly(2,5-didecyloxy-1,4-phenylenevinylene) (DOPPV).

Details about the synthesis of PPDOT and DOPPV are described elsewhere [33, 34]. The molecular weights and PDIs for both PPDOT and DOPPV as measured by GPC using polystyrene standards are given in Table 1.

**Table 1.** Molecular weight parameters, unit cell parameters and fiber extrusion temperatures $T_{ext}$ for DOPPV and PPDOT.

| | $M_w$ (kg/mol) | PDI | $T_{ext}$ (°C) | **a** (nm) | **b** (nm) | **c** (nm) | $\gamma$ |
|---|---|---|---|---|---|---|---|
| PPDOT | 95 | 6.5 | 120 | 1.89 | 0.73 | 1.18 | 90° |
| DOPPV | 4.5 | 1.3 | 70 | 2.12 | 0.80 | 0.64 | 95° |

### 2.2. Fiber Preparation by Capillary Extrusion

Oriented fibers for the PPDOT member are produced using a home built ram extruder (Figure 2) allowing processing of small amount of samples (≈ 200 mg) with defined temperature and shear rate $\dot{\gamma}$. The polymer was fed to a cylindrical reservoir which was heated to the required processing temperature. The upper plate of the extruder unit (to which the ram is attached) was coupled to the clamps of an universal testing machine (Zwick Z010) operated in compression mode with a defined speed. The corresponding shear rate was then calculated based on the capillary dimensions and the ram speed. Fibers were prepared using the ram extruder at given temperatures and shear rates: T = 120 °C; $\dot{\gamma}$ = 600 $s^{-1}$ and T = 70 °C; $\dot{\gamma}$ = 100 $s^{-1}$ for PPDOT and DOPPV, respectively. The choice of processing temperatures for preparing fibers was based on the specific modifications present in PPDOT and DOPPV. For PPDOT, the stability range of modification B ends within the temperature range T = 75–100 °C. Above T = 110 °C only modification A is observed [13]. Modification A transforms to a liquid crystalline state at about T = 170 °C followed by the complete melting between T = 210–230 °C as revealed from the DSC and temperature dependent XRD measurements [13, 32].

For DOPPV, modification B occurs in a wide temperature range but the major phase at room temperature is modification A which disappears in the temperature range T = 50–100 °C. The melting of modification B is completed at T = 210 °C. This isotropization temperature is taken from the temperature dependent intensity of the $q^B_{100}$ reflection in XRD measurements. Note that in both samples fibers have been extruded starting from a state with pre-existing small fraction of tiny crystals which probably guide the crystal growth during the subsequent processing procedure.

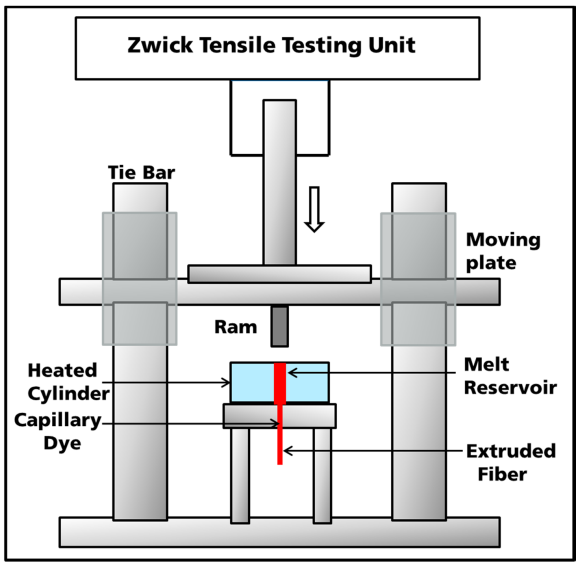


**Figure 2.** Schematic of the lab scale mini extruder used for preparing oriented fibers.

### *2.3. X-ray Scattering*

X-ray diffraction measurements in reflection mode on isotropic samples were performed using an Empyrean diffractometer (PANalytical) equipped with the temperature chamber TTK 450 (Anton Paar). The emitted CuK$\alpha$ radiation is parallelized and monochromatized using a parallel beam mirror ($\lambda$ = 1.54 Å). The scattered intensity passes a parallel plate collimator (0.27°) and is detected by a Pixel detector with 19 channels of 0.055 $\mu$m size combined to be used as a receiving slit. The scan range was 1.5 $nm^{-1} \leq q \leq 20.0\ nm^{-1}$, the step size 0.05° and the counting time per step 1 s.

X-ray diffraction measurement on oriented fibers are performed (i) in the intermediate scattering vector range and (ii) in the WAXS range using a micro-focus radiation source and a PILATUS detector in transmission. The samples were measured in such a way that the X-ray beam was perpendicular to the extrusion direction/fiber axis. The complete scattering vector range was $1.5\ nm^{-1} \leq q \leq 20\ nm^{-1}$. CuK$\alpha$ radiation was used ($\lambda$ = 1.54 Å) and the calibration was performed using a silver behenate standard.

## 3. Results

*PPDOT*. The 2D scattering patterns and the integrated scattering profiles for PPDOT extruded fibers measured at room temperature in the intermediate and WAXS range are shown in Figure 3a and b respectively. A Bragg reflection at a scattering vector $q^A_{100} = 3.32\ nm^{-1}$ along with higher order

reflections $q^A_{200}$ and $q^A_{300}$ can be observed indicating a long range ordered lamellar state. The relevant inter-planar spacing is $d^A_{100}$ = 18.9 Å as calculated from the peak position of the first order peak $q^A_{100}$ using Bragg's equation, d = $2\pi$/q. This lamellar structure corresponds to a periodic arrangement of nanodomains formed by rigid backbones (comprising of aromatic rings) and aggregated side chains. The obtained spacing is in good agreement with previously reported values for modification A in PPDOT [7]. The scattering pattern for PPDOT has been indexed assuming an orthorhombic unit cell [13]. The reflection indexed as $q^A_{020}$ at q ≈ 17.3 nm$^{-1}$ corresponds to an interplanar spacing $d^A_{020}$ of about 3.65 Å and is related to the distance between the aromatic rings within the stacks of main chains ($\pi - \pi$ spacing). The peak at q = 5.3 nm$^{-1}$ with an interplanar spacing $d^A_{001}$ of about 11.9 Å corresponds to the periodicity (or side chain-to-side chain distance) in main chain direction. Presence of a small fraction of modification B is revealed by the presence of a Bragg reflection at scattering vector q, $q^B_{100}$ = 4.6 nm$^{-1}$ corresponding to the inter-lamellar spacing ($d^B_{100}$ = 13.6 Å). The detailed analysis can be found elsewhere [13]. Importantly, anisotropic intensity distribution is observed for the above mentioned reflections indicating a preferred orientation. Intensity maximum along the equatorial position for the $q^A_{100}$ peak corresponding to the layered morphology and along the meridional position for the $q^A_{001}$ peak implying that the surface normals of the respective lattice planes are orthogonal to each other (insets of Figure 3a and b). Further, the 2D WAXS pattern (inset Figure 3b) exhibits an intensity maximum along the equatorial position for the reflection at $q^A_{020}$ ≈ 17.3 nm$^{-1}$ corresponding to the $\pi - \pi$ stacking. The observed 2D pattern indicate that the lamella related to the $q^A_{100}$ reflections have surface normal which are preferentially oriented perpendicular to the fiber axis and that the polymer backbones align along the extrusion direction while the side chains align perpendicular to the extrusion direction. Interestingly, the orientation of modification A and B fractions in extruded PPDOT samples is practically identical. This is expected if modification B is formed starting from modification A by a solid-solid transition [13].

*DOPPV*. The 2D scattering patterns and the integrated intensity profiles for DOPPV extruded fibers measured at room temperature in the intermediate and WAXS range are shown in Figure 3c and d respectively. In the intermediate scattering range, two Bragg reflections at scattering vectors q ≈ 2.35 nm$^{-1}$ (labeled as $q^A_{100}$) and q ≈ 2.9 nm$^{-1}$ (labeled as $q^B_{100}$) can be observed suggesting probably the presence of two polymorphic states, i.e., modifications A and B. The interplanar spacings are $d^A_{100}$ = 26.7 Å and $d^B_{100}$ = 21.6 Å as calculated from the peak positions of the first order peak. Interestingly, higher order reflections $q^B_{200}$ and $q^B_{300}$ are only observed for the polymorphic state B indicating a lamellar structure. The absence of higher order reflections ($q^A_{200}$, $q^B_{300}$) and a relatively smaller coherence length $l^A_{100}$ ≈ 75 Å (calculated using Scherrer's equation; $l = 2\pi$/FWHM) as compared to $l^B_{100}$ ≈ 305 Å suggests that the polymorphic state A is not significantly long-range ordered. Previously, the scattering pattern for the octyl member (C = 8) for AOPPVs has been indexed using a monoclinic unit cell [35, 36]. The reflection indexed as $q^A_{020}$ at q ≈ 13.5 nm$^{-1}$ and $q^B_{020}$ at q ≈ 15.5 nm$^{-1}$ corresponds to an interplanar spacing $d^A_{020}$ of about 4.65 Å and $d^B_{020}$ of about 4.05 Å and is related to the distance between the aromatic rings within the stacks of main chains ($\pi - \pi$ spacing). A weak shoulder at q ≈ 10 nm$^{-1}$ with an interplanar spacing $d^B_{001}$ of about 6.3 Å corresponds to the periodicity (side chain-to-side chain distance) in main chain direction [36]. Similar to PPDOT fibers, anisotropic intensity distribution is observed in the 2D scattering patterns for DOPPV fibers indicating a preferred orientation. In clear contrast to the PPDOT fibers, the 2D scattering pattern of DOPPV fibers seem to exhibit a different molecular orientation. The Bragg reflections $q^A_{100}$ and $q^B_{100}$ show intensity maximum

along the equatorial position. Like in PPDOT the lamellae related to the $q^{A}_{100}$ peak have surface normals which are oriented perpendicular to the shear direction/fiber axis. The Bragg reflections corresponding to the $\pi - \pi$ stacking ($q^{A}_{020}$ and $q^{B}_{020}$) exhibit intensity maxima along the meridional position supporting that the $\pi - \pi$ stacks preferentially orient with the surface normals along the fiber axis, i.e., the backbones are oriented perpendicular to the extrusion direction. Note that similar results were obtained on the extruded fibers of other members of the AOPPVs series with varying side chains having C = 8 and C = 12.

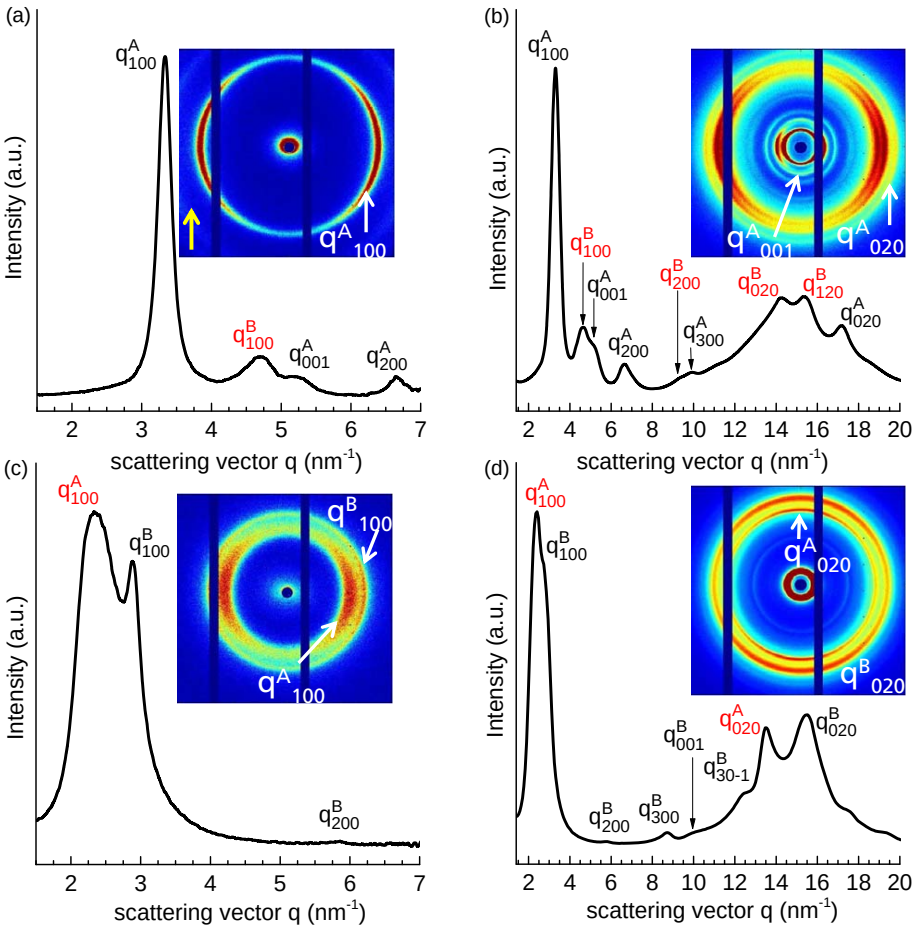


**Figure 3.** 2D scattering patterns of the extruded fibers for PPDOT (a, b) and DOPPV (c, d) in the intermediate (a, c) and WAXS (b, d) range along with the corresponding integrated scattering profiles. Important Bragg peaks are marked. The fiber is placed in such a way that it is vertical and lying in the plane of paper. The shear direction (fiber axis) is marked with a yellow arrow. Intensity maximum is seen at the equatorial positions for the (100) Bragg peaks for both DOPPV and PPDOT. However, meridinonal scattering is stronger in the case of (020) Bragg peak for DOPPV while, for PPDOT the (020) Bragg peak shows intensity maximum along the equatorial position indicating different backbone packing in DOPPV and PPDOT. The black regions (rectangular stripes) in the images are due to the blind areas of the detector.

An important aspect that needs to be investigated is whether there is any influence of processing

on the overall structural packing. The scattering profiles of PPDOT and DOPPV on isotropic samples at room temperature after cooling from the melt state are shown in Figure 4a and b respectively. A comparison of the intensity profiles shown in Figure 3 and Figure 4 for PPDOT and DOPPV reveals that there is no measurable influence of extrusion processing on the lamellar morphology with almost constant interlamellar spacing for both PPDOT and DOPPV. The only major difference is that PPDOT samples cooled from melt predominantly exhibit modification A with smaller $q^A_{100}$ (modification B with larger $q^B_{100}$ is absent). However, it has been shown that long storage of PPDOT under ambient conditions lead to a partial conversion of modification A to B [13]. The crystallographic structure of both PPDOT and DOPPV can be analyzed in detail based on the X-ray diffraction pattern taken from powder-like and oriented samples. The scattering pattern for PPDOT (Figure 4a) can be indexed assuming an orthorhombic unit cell with lattice parameters a = 1.89 nm, b = 0.73 nm and c = 1.18 nm while DOPPV (Figure 4b) can be indexed by a monoclinic unit cell with lattice parameters a = 2.12 nm, b = 0.804 nm and c = 0.64 nm and $\gamma = 95°$.

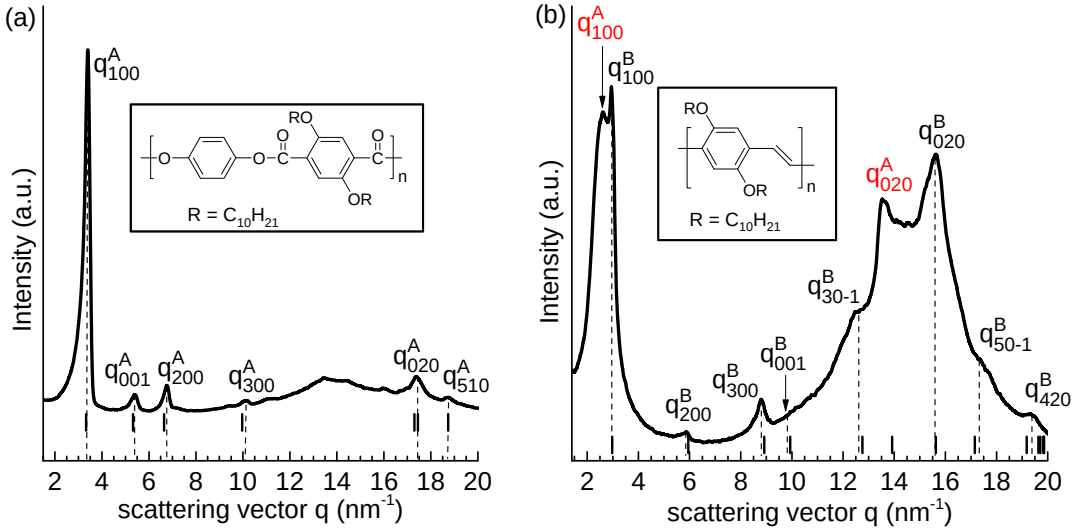


**Figure 4.** Scattering patterns for isotropic samples of (a) PPDOT (modification A) and (b) DOPPV (preferentially modification B) measured at room temperature after a stepwise cooling from the melt state along with peak indexing using an orthorhombic and a monoclinic unit cell for PPDOT and DOPPV respectively. The Bragg peaks marked in red in (b) corresponds to the polymorphic state modification A which is not really long range ordered.

## 4. Discussion

Based on the results shown in the preceding section, the most important facet of this study is that molecular orientation can be achieved in extruded fibers of comb-like polymers with rigid backbones (PPDOT and DOPPV) under the influence of shear fields with well defined processing conditions (temperature and shear forces). Both PPDOT and DOPPV show two different polymorphic states characterized by a lamellar morphology with alternating main chain and alkyl nanodomains (for DOPPVs only modification B clearly exhibits a lamellar morphology). Such a behavior is obviously a

general feature and has been observed for various series of comb-like polymers [8]. The interesting finding in the investigated comb-like polymers is the different orientation of rigid backbones in the shear fields despite of an uniform orientation of the (100) lamellae. This is supported by the difference in the position of anisotropic intensity distribution between the (100) and (020) reflections for PPDOT and DOPPV as observed in the 2D scattering patterns (Figure 3). While for PPDOT the polymer backbones align along the extrusion direction (fiber axis), for DOPPV the polymer backbones stack perpendicular to the extrusion direction. A schematic of the backbone packing in PPDOT and DOPPV shear extruded fibers based on the results obtained from the 2D scattering measurements is shown in Figure 5. The question arises what is causing a difference in the orientation of the backbone packing under the influence of shear fields.

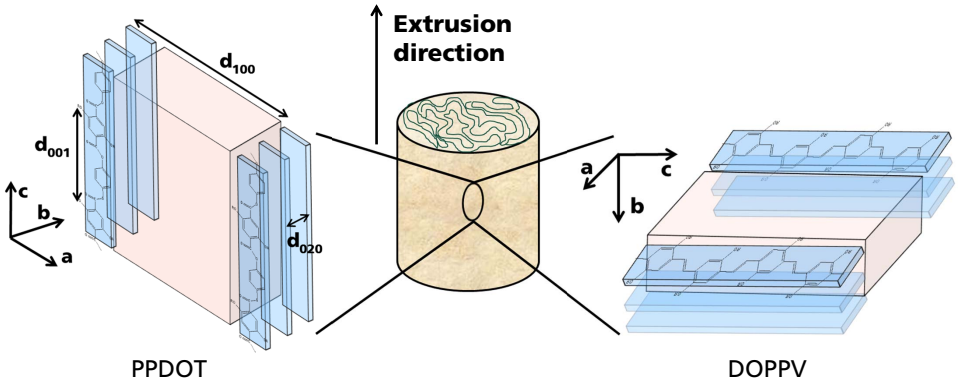


**Figure 5.** Schematic of preferred molecular orientation in extruded fibers of PPDOT and DOPPV under shear fields. While for PPDOT the rigid polymeric backbones orient along the extrusion direction, for DOPPV the polymeric backbones orient perpendicular to the extrusion direction preserving the in plane lamellar morphology.

A major difference between PPDOT and DOPPV is that there are significant differences in the packing state of the side chains within the alkyl nanodomains. The detailed crystallographic structure analysis of both PPDOT and DOPPV on the basis of the X-ray diffraction pattern taken from powder-like and oriented samples shows that there are significant differences in the lattice parameters of PPDOT and DOPPV (Table 1). This can be understood as a first indication for differences regarding the packing state of the side chains. Recently, a detailed model-free analysis to determine the packing state of the methylene sequences in the alkyl nanodomains has been proposed based on the calculation of the average volume per $CH_2$ unit, $V_{CH2}$, using the lattice parameters obtained from scattering measurements [13, 35]. The results for PPDOT samples containing modification A reveal that the side chains are amorphous/disordered within the alkyl nanodomains with the $V_{CH2}$ values close to that for amorphous polyethylene. On the contrary, the situation in DOPPV samples containing modification B is quite different. Here, the average volume per $CH_2$ unit is much smaller and even below the value expected for crystalline polyethylene.[34] Such a high packing density of the methylene sequences implies a high degree of crystallinity within the alkyl nanodomains. Figure 6 shows the unit cell packing with amorphous/disordered and crystalline packing of side chains within the alkyl nanodomains for PPDOT and DOPPV respectively. We hypothesize that the modification-dependent differences in the $V_{CH2}$ value is a possible reason for a different orientation of backbones under the influence of shear fields. Further, it is also known from studies on block

copolymers that a general change in orientation can occur at a certain threshold in the shear rate dependence [37, 38]. Although, experiments conducted with different shear rates on extruded PPDOT fibers revealed no threshold shear rate for a possible orientation inversion, it will be interesting to see whether the orientation in DOPPV fibers have any shear rate and temperature dependence.

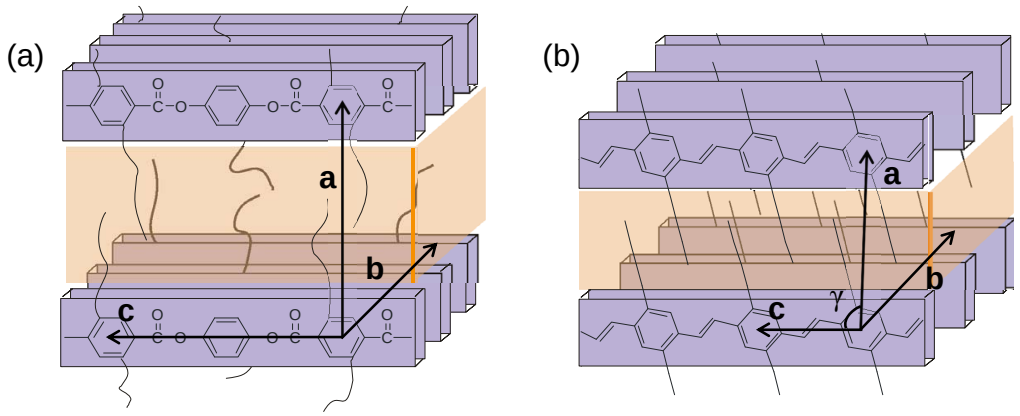


**Figure 6.** Schematic of the unit cell structure of (a) PPDOT (disordered side chains) and (b) DOPPV (crystalline side chains).

Irrespective of the mechanism, it is important to note that an oriented morphology can be achieved in extruded fibers by shear fields in well reproducible and relatively easy way. Common approaches like friction transfer [36], fiber spinning [39] or by magnetic fields [40] have often certain limitations. From this perspective, achieving orientation in comb-like polymers by shear fields with well defined processing conditions presents a simple, robust and efficient approach to obtain oriented crystals.

## 5. Conclusion

In summary, we have shown that both poly(1,4-phenylene-2,5-didecyloxy terephthalate) (PPDOT) and poly(2,5-didecyloxy-1,4-phenylenevinylene) (DOPPV) exhibit a nanophase separated layered morphology. 2D X-ray scattering results on extruded fibers exhibit a preferred morphological orientation with the polymeric backbones orienting along (PPDOT) and perpendicular (DOPPV) to the extrusion direction. Further, there is no effect of shear processing on the overall unit cell structure and layered morphology as revealed by measurements on isotropic samples of individual polymers. While, PPDOT packs on orthorhombic unit cell, the unit cell packing for DOPPV is monoclinic. The different orientation of the backbones under shear fields could possibly be originating from the different packing of the alkyl side chains within the alkyl nanodomains which are crystalline and disordered for DOPPV and PPDOT respectively.

## Acknowledgments

Financial support by the DFG in the framework of the SFB/TRR102 *"Polymers under multiple constrains: restricted and controlled molecular order and mobility"* (project B14) is acknowledged. The authors thank the Experimental Polymer Physics group of Thomas Thurn-Albrecht for a fruitful collaboration regarding X-ray diffractometry measurements on polymers within the SFB/TRR 102.

## Conflict of Interest

The authors declare no competing financial interest.

## References


1. Heeger AJ (2001) Semiconducting and metallic polymers: The fourth generation of polymeric materials. *J Phys Chem B* 105: 8475–8491.
2. Ong BS, Wu YL, Liu P, et al. (2004) High-performance semiconducting polythiophenes for organic thin-film transistors. *J Am Chem Soc* 126: 3378–3379.
3. Blom PWM, Vissenberg MCJM (2000) Charge transport in poly(p-phenylene vinylene) light-emitting diodes. *Mater Sci Eng R* 27: 53–94.
4. Gallot B (1996) Comb like and block liquid crystalline polymers for biological applications. *Prog Polym Sci* 21: 1035–1088.
5. Jianquan T, Weiqu L, Honglei W, et al. (2016) Preparation and properties of UV-curable waterborne comb-like(meth)acrylate copolymers with long fluorinated side chains. *Prog Org Coat* 94: 62–72.
6. Jackson WJ (1980) Liquid crystal polymers. IV. Liquid crystalline aromatic polyesters. *Brit Poly J* 12: 154–162.
7. Ballauf M (1989) Stiff-chain polymers—Structure, phase-behavior, and properties. *Angew Chem Int Ed Engl* 28: 253–267.
8. Shi H, Zhao Y, Dong X (2013) Frustrated crystallization and hierarchical self-assembly behavior of comb-like polymers. *Chem Soc Rev* 42: 2075–2099.
9. Beiner M, Huth H (2003) Nanophase separation and hindered glass transition in side-chain polymers. *Nat Mater* 2: 595–599.
10. Pankaj S, Beiner M (2010) Confined dynamics and crystallization in self-assembled alkyl nanodomains. *J Phys Chem B* 114: 15459–15465.
11. Zheng W, Levon K, Laakso J, et al. (1994) Characterization and solid-state properties of processable N-alkylated polyanilines in the neutral state. *Macromolecules* 27: 7754–7768.
12. Watanabe J, Ono H, Uematsu I, et al. (1985) Thermotropic polypeptides. 2. Molecular packing and thermotropic behavior of poly(L-glutamates) with long n-alkyl side chain. *Macromolecules* 18: 2141–2148.
13. Gupta G, Danke V, Babur T, et al. (2017) Interrelations between side chain and main chain packing in different crystal modifications of alkoxylated polyesters. *J Phys Chem B* 121: 4583–4591.
14. Sirringhaus H, Brown PJ, Friend RH, et al. (1999) Two-dimensional charge transport in self-organized, high-mobility conjugated polymers. *Nature* 401: 685–688.
15. Gargi D, Kline RJ, DeLongchamp DM, et al. (2013) Charge transport in highly face-on poly(3-hexylthiophene) films. *J Phys Chem C* 117: 17421–17428.

16. Koynov K, Bahtiar A, Ahn T, et al. (2006) Molecular weight dependence of chain orientation and optical constants of thin films of the conjugated polymer MEH-PPV. *Macromolecules* 39: 8692–8698.

17. Hamaguchi M, Yoshino K (1995) Rubbing-induced molecular orientation and polarized electroluminescence in conjugated polymer. *Jpn J Appl Phys* 34: 712–715.

18. Okuzaki H, Hirata Y, Kunugi T (1999) Mechanical properties and structure of zone-drawn poly(p-phenylene vinylene) films. *Polymer* 40: 2625–2629.

19. Lin NT, Satyanarayana K, Chen CH, et al. (2014) Controlling the orientation of pendants in two-dimensional comb-like polymers by varying stiffness of polymeric backbones. *Macromolecules* 47: 6166–6172.

20. Jeng U, Hsu CH, Sheu HS, et al. (2005) Morphology and charge transport in poly(2-methoxy-5-(2'-ethylhexyloxy)-1,4-phenylenevinylene) films. *Macromolecules* 38: 6566–6574.

21. Singh CR, Gupta G, Lohwasser R, et al. (2013) Correlation of charge transport with structural order in highly ordered melt crystallized P3HT films. *J Polym Sci Part B Polym Phys* 51: 943–951.

22. Brinkmann M, Contal C, Kayunkid N, et al. (2010) Highly oriented and nanotextured films of regioregular poly(3-hexylthiophene) grown by epitaxy on the nanostructured surface of an aromatic substrate. *Macromolecules* 43: 7604–7610.

23. Kim JS, Park Y, Lee DY, et al. (2010) Poly(3-hexylthiophene) nanorods with aligned chain orientation for organic photovoltaics. *Adv Funct Mater* 20: 540–545.

24. Fischer FSU, Tremel K, Sommer M, et al. (2012) Directed crystallization of poly(3-hexylthiophene) in micrometre channels under confinement and in electric fields. *Nanoscale* 4: 2138–2144.

25. Ebert F, Thurn-Albrecht T (2003) Controlling the orientation of semicrystalline polymers by crystallization in magnetic fields. *Macromolecules* 36: 8685–8694.

26. Freidzon YAS, Talroze RV, Boiko NI, et al. (1988) Thermotropic liquid-crystalline polymers XXIII. Peculiarities of uniaxial orientation of comb-like liquid-crystalline polymers under mechanical stress. *Liq Cryst* 3: 127–132.

27. Nagamatsu S, Takashima W, Kaneto K (2003) Backbone arrangement in friction-transferred regioregular poly(3-alkylthiophene)s. *Macromolecules* 36: 5252–5257.

28. Hamidi-Sakr A, Biniek L, Fall S, et al. (2016) Precise control of lamellar thickness in highly oriented regioregular poly(3-hexylthiophene) thin films prepared by high-temperature rubbing: Correlations with optical properties and charge transport. *Adv Funct Mater* 26: 408–420.

29. Rim YS, Bae SH, Chen HJ, et al. (2016) Recent progress in materials and devices toward Printable and flexible sensors. *Adv Mater* 28: 4415–4440.

30. Reinspach JA, Diao Y, Giri G, et al. (2016) Tuning the morphology of solution-sheared P3HT:PCBM films. *ACS Appl Mater Interfaces* 8: 1742–1751.

31. Rauwendaal C (2001) *Polymer Extrusion*, Carl Hanser Verlag Munich.

32. Damman SB, Vroege GJ (1993) Liquid-crystalline main-chain polymers with a poly(p-phenylene terephthalate) backbone. X-ray-diffraction of the polyester with dodecyloxy side-chains. *Polymer* 34: 2732–2739.

33. Babur T, Balko J, Budde H, et al. (2014) Confined relaxation dynamics in long range ordered polyesters with comb-like architecture. *Polymer* 55: 6844–6852.

34. Babur T (2017) Structure and relaxation dynamics of comb-like polymers with rigid backbone [PhD Dissertation]. Martin Luther University Halle-Wittenberg.

35. Babur T, Gupta G, Beiner M (2016) About different packing states of alkyl groups in comb-like polymers with rigid backbones. *Soft Matter* 12: 8093–8097.

36. Nagamatsu S, Misaki M, Chikamatsu M, et al. (2007) Crystal structure of friction transferred poly(2,5-dioctyloxy-1,4-phenylenevinylene). *J Phys Chem B* 111: 4349–4354.

37. Balsara NP, Dai HJ (1996) A transition from shear-induced order to shear-induced disorder in block copolymers. *J Chem Phys* 105: 2942–2945.

38. Vigild ME, Chu C, Sugiyama M (2001) Influence of shear on the alignment of a lamellae-forming pentablock Copolymer. *Macromolecules* 34: 951–964.

39. Damman SB, Mercx FPM (1993) About different packing states of alkyl groups in comb-like polymers with rigid backbones. *J Polym Sci Part B Polym Phys* 31: 1759–1767.

40. Falk U, Westermark B, Boeffel C, et al. (1987) NMR of stiff macromolecules with flexible side chains. *Mol Cryst Liq Cryst* 153: 199–206.


AIMS Press